Journal Pre-proof

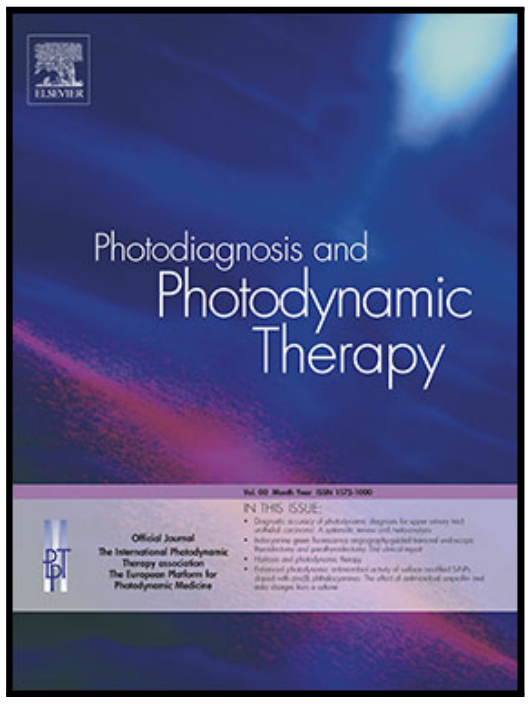

Topographic correlation of retinal vascularity and electrophysiology in Nepalese high myopes: Insights for early detection and monitoring

Bipin Koirala , Parash Gyawali , Manoj Mahat , Krishna Gurung , Punay Pratap Sah , Gauri Shankar Shrestha

PII: S1572-1000(25)00796-3
DOI: https://doi.org/10.1016/j.pdpdt.2025.105265
Reference: PDPDT 105265

To appear in: *Photodiagnosis and Photodynamic Therapy*

Received date: 19 August 2025
Revised date: 8 October 2025
Accepted date: 24 October 2025

Please cite this article as: Bipin Koirala , Parash Gyawali , Manoj Mahat , Krishna Gurung , Punay Pratap Sah , Gauri Shankar Shrestha , Topographic correlation of retinal vascularity and electrophysiology in Nepalese high myopes: Insights for early detection and monitoring, *Photodiagnosis and Photodynamic Therapy* (2025), doi: https://doi.org/10.1016/j.pdpdt.2025.105265

Highlights:

- In High myopes, multifocal electroretinography (mfERG) parameters correlate with Optical Coherence Tomography Angiography (OCTA) parameters in parafoveal and perifoveal retinal zones.
- mfERG and OCTA parameters show differential sensitivity in tracking myopic axial length elongation in different retinal loci
- In the foveal region, only N1 implicit time (AUC = 0.701) showed good sensitivity in tracking myopic axial length elongation.
- In the perifoveal region, DCP-VD (AUC = 0.71), P1 implicit time (AUC = 0.704) and N1 implicit time (AUC = 0.708) demonstrated good sensitivity in tracking myopic axial length elongation.
- In the parafoveal region, SCP-VD (AUC = 0.693) and N1 implicit time (AUC = 0.680) demonstrated average sensitivity in detecting myopic axial length elongation.

Topographic correlation of retinal vascularity and electrophysiology in Nepalese high myopes: Insights for early detection and monitoring

Bipin Koirala[1], Parash Gyawali[2], Manoj Mahat[2], Krishna Gurung[1], Punay Pratap Sah[1], Gauri Shankar Shrestha[2]

[1]Pokhara University, Pokhara, Nepal

[2]Maharajgunj Medical Campus, Institute of Medicine, Tribhuvan University, Nepal

Running Title: Retinal Vascularity and Electrophysiology in High Myopia

Corresponding Author:

Parash Gyawali, parash.gyawali619@gmail.com

ORCID iD: https://orcid.org/0000-0003-1201-4234

Disclosure: The authors report no conflicts of interest and have no proprietary interest in any of the materials mentioned in this article.

Acknowledgement:

All the participants of this study.

Keywords: High Myopia, Optical Coherence Tomography Angiography (OCTA), Multifocal Electroretinography (mfERG), Axial Length, Retinal Vessel Density

ABSTRACT

Background: mfERG and OCTA parameters have been widely used in myopes to study retinal changes in the myopic retina. However, this study addresses, for the first time, the sensitivity of mfERG and OCTA in tracking myopic axial length changes.

Methods: Forty high myopes (mean spherical equivalent, MSE ≥ -6.00D) and 40 age- and sex- matched emmetropes (MSE=0.00D) underwent a comprehensive eye examination, including ocular biometry, OCTA for assessment of superficial capillary plexus vessel density (SCP-VD) and deep capillary plexus vessel density (DCP-VD), and mfERG for measuring N1 and P1 amplitude and implicit time. Correlation between mfERG and OCTA parameters was evaluated by comparing Ring1, Ring 2 and Ring 3 mfERG parameters with foveal, parafoveal (3 mm) and perifoveal (6 mm) OCTA parameters, respectively. Receiver Operating Characteristics (ROC) curve analysis was performed to calculate the sensitivity of mfERG and OCTA parameters in tracking myopic axial length elongation in different retinal loci.

Results: In high myopes, mfERG amplitudes and implicit time exhibited a significant positive and negative correlation, respectively, with OCTA parameters in perifoveal and parafoveal zones. In the foveal region, N1 implicit time (AUC= 0.701), in the perifoveal region, DCP-VD (AUC = 0.71), P1 implicit time (AUC = 0.704) and N1 implicit time (AUC = 0.708) demonstrated good sensitivity whereas, in the parafoveal region, SCP-VD (AUC = 0.693) and N1 implicit time (AUC = 0.680) demonstrated average sensitivity in detecting axial length elongation.

Conclusion: We infer that mfERG and OCTA parameters show differential sensitivity in tracking axial length elongation in different retinal loci and could serve as tools for myopia management.

Introduction

Myopia is the most prevalent refractive error and a significant global public health challenge.[1,2] Currently, approximately 28.3% of the global population is affected by myopia, and 4.0% have high myopia. By 2050, these figures are expected to rise to 49.8% for myopia and 9.8% for high myopia.[1] High myopia is a refractive error with a spherical equivalent ≥ −6.00 Diopter or an axial length > 26.00 mm.[2] High myopia, which often progresses to pathological myopia, can cause serious, sight-threatening retinal complications.[2] Currently, pathological myopia has caused visual impairment or blindness in 0.1 - 0.5% of Caucasians and 0.2 - 1.4% of Asians, with these rates expected to increase alongside the projected rise in myopia prevalence.[3]

The underlying causes of myopia remain unclear, although associations with genetic factors, the level of outdoor activities, ultraviolet (UV) exposure, and near work activities suggest that multiple factors contribute to its development.[2] Excessive axial elongation is a primary pathophysiological feature in high myopia, often resulting in the thinning of the retina, choroid[4] and sclera.[2] This retinal thinning results in a reduction in the densities of photoreceptors, retinal pigment epithelium, and other retinal cells, particularly in the equatorial and retro-equatorial zones, consequently compromising retinal function compared to the emmetropic eyes.[2,5]

Blood vessels are the major route for supplying oxygen and nutrients to retinal cells; any disruptions in the supply and demand balance can contribute to various retinal disorders, including high myopia.[6] Studies indicate that high myopic eyes undergo various microvascular changes such as altered vessel density, blood flow and vascular caliber, which may contribute to the pathogenesis of myopia.[7,8] Understanding these retinal microvasculature alterations is key to recognising early anatomical changes and assessing potential risks of visual impairment in high myopia[7, 9–11]

Optical Coherence Tomography Angiography (OCTA) is non-invasive imaging modality instrumental in detecting abnormal vascular changes in various retinal conditions, including high myopia.[11,12] Multifocal electroretinography (mfERG) helps in early detection of

alterations in retinal function by analysing the biphasic first-order kernel.[13,14] In high myopia, studies suggest a significant decrease in amplitude density and prolongation of implicit time of both N1 and P1 waves.[14] These findings highlight the sensitivity of mfERG to detect functional impairments in myopic retina, emphasizing its potential role in monitoring early retinal changes associated with axial elongation.

Retinal imaging using OCTA and electrophysiological assessment via mfERG are widely utilised in myopia research. However, the literature does not provide information on the sensitivity of OCTA and mfERG in tracking axial length elongation. Axial length is a key ocular biometric parameter commonly used to monitor myopia progression. In this study, we examine the sensitivity of OCTA and mfERG parameters across different retinal loci for tracking axial length elongation. Myopic axial elongation differentially affects vessel density [15] and electrophysiological responses across retinal loci. [16] Functional variations are also age-dependent, with foveal impairment noted in children and paracentral reduction in adults.[16] Given these regional susceptibilities, exclusive focus on the foveal zone may underestimate early changes. Therefore, monitoring both vascular and electrophysiological alterations across different retinal loci can inform targeted interventions. If one myopia control modality fails to preserve retinal integrity, alternative strategies should be explored.

Additionally, this study presents a topographical analysis of OCTA and mfERG parameters across various retinal zones, providing insights into regional differences within the macular area in high myopic eyes. Hence, our approach could improve understanding of how specific retinal loci are impacted in high myopia, which could add evidence and guidance for refinement of intervention strategies.[17]

Methods

Study Design and Participants

This cross-sectional, comparative study included 80 participants, divided into 40 high myopes and 40 emmetropes. Purposive sampling was conducted over nine months at the Himalayan Eye Hospital, Pokhara, Nepal. This study adhered to the Tenets of the Declaration

of Helsinki and was approved by the Institutional Review Committee, Pokhara University (Protocol no: 183-2080/81). Inclusion criteria for high myopes were aged between 18 -30 years, mean spherical equivalent (MSE) of -6.00 D or greater (defined as spherical plus half of cylinder power) after cycloplegic refraction and axial length greater than or equal to 26.00 mm. Only the eye with the greater refractive error from each participant was included in the study and underwent OCTA, followed by mfERG. For comparison, healthy emmetropes with an MSE within ± 0.50D, and matched for age and gender, were enrolled. Exclusion criteria included pathological myopia or any other ocular disease other than myopia, vitreoretinal diseases, systemic vascular diseases and history of prior ocular surgeries, including refractive and vitreoretinal procedures.

Clinical profile Assessments

A detailed ocular examination was performed on each eye, which involved assessing visual acuity with a logMAR chart at 4-meter distance, objective and subjective refraction and slit lamp bio-microscopy using a slitlamp (Topcon SL-D4, Japan). A dilated fundus examination was carried out using a Volk +90D lens on slit lamp biomicroscope a Volk +20D lens was used for indirect ophthalmoscopy. Biometric data (axial length and keratometry) were obtained using the Nidek AL-Scan optical biometer (Nidek CO, Japan). An eye with greater refractive error from each participant was only included in the study and underwent OCTA followed by mfERG.

Optical Coherence Tomography Angiography (OCTA)

OCTA imaging was conducted with the RTVue XR Avanti spectral-domain OCT device equipped with AngioVue software (version 2015.1.1.98; Optovue, Inc., Freemont, CA, USA). The Optovue AngioVue system utilised the split-spectrum amplitude-decorrelation angiography (SSADA) algorithm. The instrument operated at a data scanning speed of 70,000 scans per second using a light source of wavelength 840 nm and a bandwidth of 50 nm. Each OCTA volume consisted of 304 × 304 A-scans with two consecutive B-scans captured at each fixed position before moving to the next sampling location. The Optovue software automatically segmented each layer and analysed the results.

Vessel density (VD) of entire macula and each specific zone (fovea, parafovea, perifovea) was calculated based on Early Treatment of Diabetic Retinopathy Study (ETDRS) map at both superficial (SCP-VD) and deeper vascular plexus levels (DCP-VD). In the study, vessel density was quantified in terms of the percentage of area occupied by retinal vessels in a specific area of 6x6 mm dimension. For vessel density quantification, OCTA images are digitised and individual pixels are classified from bright to dark, along with the use of different types of binarisation thresholding. Vessel density thus calculated in terms of percentage is not an absolute value rather relative parameter, and it can vary depending on the device used[18], image processing method[19,20], light intensity[21], pixel size[22], scan size[23]. Hence, great caution must be taken while comparing the value across devices and following a patient over time longitudinally.

The linear retinal image parameter is significantly influenced by longer axial length in high myopia. Longer axial length leads to a larger image scale, which can distort true vessel density measurements if left uncorrected, so correction was done by manual calculation. While measuring retinal vessel density, it is crucial to consider the ocular magnification effect. The magnification factor of the eye (q) was calculated using the Littmann-Bennet formula: q=0.01306 x (AL-1.82), where AL is the axial length of the eye and 1.82 is a constant[24]. The true dimension (T) is calculated as T=M x q x p where M is the measured dimension of the image, T is the true dimension and p is the magnification factor of the imaging system. The factor p can be accurately calculated using the Bennet formula if the AL at which M = T is known, and if the effects arising from image distortion are omitted. The factor p for RTVue XR Avanti OCTA instrument used in the present study is 3.48,[25] where the defined axial length for the OptovueRTVue XR Avanti system is 23.95 mm (Optovue, Inc., personal communication, 2017).[26]

According to the automated setting, the superficial network ranged from 3μm below the internal limiting membrane to 15 μm below the Inner Plexiform Layer (IPL), while the deep capillary network extended from 15 to 70 μm below IPL. Any images with signal strength below 6 were excluded. Each study subject was well instructed to maintain adequate head

position and steady fixation during scanning. A high-definition macular Angio scan (6mmX6mm) and normal retinal A-scan (6 mm X 6 mm) cube scan was performed.

Multifocal Electroretinography (mfERG)

The mfERG was conducted using the Metro Vision (MonpackONE) Electrophysiology device, following proper calibration and adherence to the International Society for Clinical Electrophysiology of Vision (ISCEV) protocol.[13] mfERG is a minimally invasive technique that has very few complications. It involves pupillary dilation, which causes slight blurring of vision, and the electrodes placed in contact with the cornea, limbus, and conjunctiva can sometimes cause corneal abrasion. Skin electrodes placed over the temple and forehead can irritate rarely. The testing duration ranges from 4 minutes for 61-element arrays to 10 minutes for 103-element arrays.[13]

The mfERG responses were recorded using a DTL electrode, placed in the lower fornix, in contact with the lower cornea along the lid margin after applying a local anesthetic drop Gold-cup reference and surface electrodes were attached to the temple and forehead, respectively. The impedance was kept below 5 k-ohm. The filter band pass was set to approximately 5–200 Hz, with a high-pass cutoff range of 3–10 Hz and a low-pass cutoff range of 100–300 Hz.

Pupil dilation to at least 7 mm was achieved using Tropicamide (0.5% w/v, Auromide, Aurolab, India), and participants were light-adapted under normal room illumination for 15 minutes before the test. The mfERG stimulus involved a high luminance, high contrast, 61-hexagon pattern array, scaled with eccentricity and positioned 33 cm from the subject, covering nearly 40-50 degrees of the central visual field. The visual stimulus array operated at a frame rate of 75 Hz, with each hexagon alternating between black and white according to a pseudorandom binary m-sequence, with luminance of 100 cd/m² for the white hexagons and 0-3 cd/m² for black hexagons in moderate room lighting (surface luminance: < 300 cd/m²).

Participants were corrected for the viewing distance, and they were instructed to maintain focus on a red fixation target at the center of the stimulus matrix. Each recording session lasted approximately 4 minutes, divided into four segments of 1 minute each. The response

density amplitude (nV/deg^2) and implicit time of N1 and P1 waveforms were measured, recorded, **(Figure 1)** and presented a trace array of 61 local retinal responses, and group trace averages for the central 3 concentric rings (Ring1 to Ring3).

Topographical correlation of mfERG rings with ETDRS grid of OCTA.

Anatomical studies have indicated that the foveola measures 0.35 mm in diameter, which corresponds to 1 degree of visual angle.**(Figure 2A)**[27] Based on this measurement, the mfERG rings were aligned with specific sections of ETDRS chart, with Ring 1 corresponded to central 1mm circle, Ring 2 aligned with parafoveal 3mm circle, and Ring 3 corresponding to perifoveal 6mm circle. This alignment enabled precise anatomical and functional correlations across different retinal locations. **(Figure 2B)**

The amplitude density and implicit time of mfERG wave components were then calculated for each ring (Ring1 to Ring 3), while retinal vessel density was measured in foveal, parafoveal, and perifoveal retinal zones using ETDRS grid. The relationship between mfERG parameters and OCTA measurements was explored and analyzed using Spearman correlation and multiple linear regressions.

Statistical Analysis

The data were analyzed using SPSS V-20(IBM Co. USA) software and MS-Excel (6.2.11 Excel 2010 (v14.0). The descriptive statistics were reported as mean and standard deviation; Mean (SD) for normally distributed data, and as median and interquartile range (IQR)for non-normal distribution. The normality of data was assessed using Shapiro-Wilk test. Differences in N1 and P1 amplitude, implicit time, retinal vessel density (SCP-VD and DCP-VD), between two study groups were assessed using t-test for normally distributed data and Mann-Whitney U test for non-normally distributed data. Pearson's correlation coefficient was used for normally distributed data, while Spearman's rank correlation was used for non-normally distributed data to assess the relationship between parameters obtained from OCT-A and mfERG. Multiple linear regressions were used to examine the association between mfERG parameters and OCTA parameters. A p-value of less than 0.05 was considered statistically significant. Receiver Operating Characteristic) curve analysis was performed to analyse sensitivity, specificity and Area under curve (AUC) values.

Results

The median age of high myopeswas21.00years (interquartile range, IQR: 5.50) and 23.00 years (IQR:4.00) for emmetropes, with no statistically significant difference between the groups (p = 0.23). Similarly, the male-to-female ratio was 23:17 for high myopes and 16:24 for emmetropes, with no significant difference (p = 0.18) in proportion between them. High myopes had a median spherical equivalence of -7.87 D (IQR: 2.38), compared to 0.00 D (IQR: 0.00) for emmetropes, with a statistically significant difference between the groups (p<0.001). The median axial length was 26.19 mm (IQR: 2.50) for high myopes and 23.12mm (IQR: 1.12) for emmetropes, indicating the significant difference in axial length between them (p<0.001). The median keratometry was 7.85 mm (IQR = 0.67) for high myopes and 7.83 mm (IQR = 0.55) for emmetropes, with no statistically significant difference between them (p=0.45) (**Table 1).** The median best corrected distance visual acuity (BCVA) was 0.00 (IQR: 0.00) logMAR in both high myopes and emmetropes.

Comparison of OCTA and mfERG parameters between high myopes and emmetropes

The mean vessel density, i.e. SCP-VD and DCP-VD were lower in high myopes compared to emmetropes across all three retinal zones. The mean difference of SCP-VD between myopes and emmetropes was 5.23% (SD: 1.42%), (p<0.001) at fovea; 5.24% (SD: 1.05%), (p <0.001) at parafovea and 4.16 % (SD: 0.89%), (p<0.001) at perifovea **(Figure 3A).** For DCP-VD, the mean difference was 3.99% (SD:1.86%), (p=0.05) at fovea; 5.48% (SD:1.08%), (p<0.001) at parafovea and 11.67% (SD: 1.61%), (p<0.001) at perifovea **(Figure 3B) (Table 2).**

The mean P1 and N1 amplitudes across all three rings (Ring1 to Ring3) were significantly lower in high myopes than in emmetropes and the mean P1 and N1 implicit time across these rings were also significantly longer in high myopes**.** The largest mean difference in P1 amplitude of 16.06 μV/degree^2 (SD:2.84 μV/degree^2), (p<0.001) and N1 amplitude of 12.76 μV/degree^2 (SD: 1.56 μV/degree^2), (p<0.001) was noted at Ring 1, between high myopes and emmetropes. Likewise, the most substantial delay in P1 implicit time was 2.90 ms (SD: 0.76 ms) (p<0.001) and N1 implicit time was 1.94 ms (SD: 0.62 ms) (p<0.001) was noted at Ring 1 in high myopes compared to emmetropes. **(Figure 4A, 4B) (Figure 5A, 5B) (Table 3)**

Topographic correlation between OCTA and mfERG parameters in Emmetropes and High Myopes

The topographical correlation involved correlating mfERG parameters at Rings 1, 2, and 3 with OCTA vessel density parameters (SCP-VD and DCP-VD) at foveal, parafoveal, and perifoveal zones in both emmetropes and high myopes separately.

For emmetropes, there was no significant correlation between the OCTA parameters and mfERG parameters in any retinal loci **(Table 4).** Similarly, for high myopes (**Table 5**), at Ring 1, no significant correlations were found between foveal vessel density parameters and Ring 1 mfERG parameters. At Ring 2, P1 amplitude showed weak positive correlation with parafoveal SCP-VD ($r = 0.34$, $p=0.03$) and moderate positive correlation with parafoveal DCP-VD ($r = 0.58$, $p<0.001$). Similarly, at Ring 3, P1 amplitude exhibited weak positive correlation with perifoveal SCP-VD ($r = 0.40$, $p=0.01$) only and no significant correlation with perifoveal DCP-VD.

Further, at both Ring 2 and 3, P1 implicit time showed no significant correlation with OCTA parameters. N1 amplitude at Ring 2 demonstrated no significant correlation with parafoveal SCP-VD and but significant weak positive correlation with parafoveal DCP-VD ($r = 0.34$, $p=0.03$). Whereas ring 3, N1 amplitudes showed a significant weak positive correlation with perifoveal SCP-VD ($r = 0.36$, $p=0.02$) and DCP-VD ($r = 0.36$, $p=0.02$). At both Ring 2 and 3, N1 implicit time showed no significant correlation with OCTA parameters.

Association between mfERG and OCTA parameters with axial length in high myopes

We performed multiple linear regression analyses to compute the association of mfERG with OCTA parameters, age and axial length. Age was not associated with any other variables, whereas axial length was significantly associated with all mfERG parameters in all 3 retinal loci except Ring 2 N1 amplitudes. Ring 1 mfERG parameters were not associated with any OCTA parameters. Similarly, Ring 2 and Ring 3 mfERG parameters showed significant association with OCTA parameters, mainly with DCP-VD **(Table 6).** Similarly, OCTA parameters were significantly associated with axial length change but not with age (**Table 7).**

Sensitivity of OCTA and mfERG in tracking axial length elongation in different retinal loci

We conducted ROC curve analysis in myopes to compute the sensitivity of OCTA and mfERG parameters in detecting criteria change of 0.1 mm axial length elongation **(Table 8**)as an increase in axial length by 0.1 mm per year or more is generally regarded as clinically significant for myopia progression.[28,29] The area under curve (AUC) generated through ROC curve analysis was compared among all the OCTA and mfERG parameters to compare the sensitivity in all retinal loci. In the foveal region (**Figure 6A**), N1 implicit time showed good sensitivity in tracking axial length elongation (AUC= 0.701, sensitivity = 56.1%, and specificity = 78.3%), which was the maximum sensitive parameter among all OCTA and mfERG parameters. In the parafoveal region (**Figure 6B**), SCP-VD (AUC = 0.693, sensitivity = 75% and specificity = 80%) and N1 implicit time (AUC = 0.680, sensitivity = 70% and specificity = 80%) demonstrated average sensitivity in detecting axial length elongation. In the perifoveal region **(Figure 6C)**, DCP-VD (AUC = 0.710, sensitivity = 75.4% and specificity = 65.2%), P1 implicit time (AUC = 0.704, sensitivity = 63.2% and specificity = 73.9%) and N1 implicit time (AUC = 0.708, sensitivity = 78.9% and specificity = 60.9%) demonstrated good sensitivity in detecting axial length elongation.

Discussion

Several studies have recommended the use of mfERG and retinal vascular OCTA parameters to track myopia progression and associated complications.[16,30] However, no studies have examined the sensitivity of both retinal vascularity and mfERG parameters within the same myopic cohort in detecting axial length elongation. Therefore, this study investigated retinal vascularity and mfERG parameters to determine the respective sensitivities in tracking axial length elongation in high myopes in different retinal loci.

Consistent with the literature, we observed that all the mfERG and OCTA parameters were significantly reduced in high myopes compared to the emmetropes.[14,31]

Inhigh myopes, this study noted a significant weak to moderate positive correlation between vessel density and mfERG amplitude at parafoveal and perifoveal zones. Whereas there was no significant correlation of mfERG implicit time with vessel density at parafoveal as well as perifoveal zones. In the foveal region, the vessel density parameter showed no significant correlation with any mfERG parameters. The lack of significant structural-functional correlation between Ring 1 mfERG parameters and foveal vessel density parameters may be explained by the presence of the foveal avascular zone. In the fovea, retinal cells mainly receive nutrients from the choroid, making them less reliant on retinal vasculature for their function compared to cells in the parafoveal and perifoveal zones.[32] However, in emmetropes, we did not observe any significant correlation between any of the mfERG and OCTA parameters in all retinal loci, which could be attributed to the narrow range of axial length in emmetropes or the absence of any pathological changes that affect the retinal vessel density and electrophysiological response.

Regression analysis revealed that DCP-VD and axial length were significantly associated with subnormal mfERG findings, while SCP-VD and age showed no significant association. The greater association of P1 and N1 amplitude to DCP-VD over SCP-VD in explaining the variation of mfERG waveform may be attributed to the anatomical location of the deep capillary plexus (DCP) and its role in nourishing the cells (bipolar, photoreceptor) responsible for generating mfERG signals.[11] The inner retinal layer, from inner nuclear layer to outer plexiform layer, receives most of its supply (including 10–15% for photoreceptors)

from DCP.[33,34] In contrast, the superficial capillary plexus (SCP), located at the retinal nerve fiber layer and composed of large arteries and veins, doesn't participate in oxygen and nutrient exchange in the retina and doesn't contribute to nourishment of mfERG-generating cells, explaining why the SCP isn't significantly associated with changes in mfERG parameters.[35]

Steigerwalt et al. reported cases of retinal ischemia in high myopia, suggesting that retinal hypoxia or ischemia due to hypoperfusion may be a potential cause of subnormal ERG responses.[36] Therefore, the impairment of mfERG parameters observed in high myopes in our study, despite the absence of obvious pathology[17], could also be attributed to the influence of subtle hypoxia on retinal cells as a result of reduced DCP-VD. Besides hypoxia or ischemia, a reduction in retinal cellular density may also have a parallel impact on mfERG responses.[9,34,37–42]

Klemp et al.'s study has revealed that hypoxia can significantly reduce mfERG amplitude only, while not affecting implicit time. However, ischemia can significantly impact both amplitude and implicit time.[43]In this study, the presence of subtle hypoxia but the absence of significant ischemia in high myopes likely explains the presence of significant association and correlation between mfERG amplitude and vessel density parameters, and also the absence of significant association and correlation between mfERG implicit time and vessel density parameters. This is probably due to the inclusion of high myopes without retinal pathology, where ischemia is less likely, but subtle hypoxia might be present.

Hence, based on the evidence presented, this study proposes that there is the possibility of subtle hypoxia in the middle-inner retina, even in high myopic participants without visible pathological changes. Also, alterations observed in mfERG and OCTA parameters in high myopes, even in the absence of overt pathology, could serve as an early precursor to myopic macular degeneration as long-term hypoxia and ischemia are often linked as primary factors driving the pathological changes seen in the retina in the case of pathological myopia.[44]

The ROC curve analysis demonstrated that N1 implicit time had good ability in detecting axial length elongation in the foveal region, whereas other mfERG and retinal vascular

parameters demonstrated poor (AUC < 0.6) axial length elongation detection. Similarly, in the parafoveal region SCD-VD and the perifoveal region DCP-VD, P1 implicit time and N1 implicit time demonstrated good ability (AUC > 0.70) in detecting axial length elongation. Our ROC curve analysis suggests that monitoring of N1 implicit time in the foveal region, SCP-VD in the parafoveal region and DCP-VD, P1 implicit time and N1 implicit time in the perifoveal region could be a good indicator of myopic axial length elongation. These ROC curve analysis findings could provide insights into optimizing myopia treatment strategies, comparing the efficacy of available myopia treatment interventions, tracking myopia progression and could serve as an early sign or sensitive biomarker of impending complications like myopic macular degeneration and other blinding pathological retinal changes[11,16,45]

The ability to predict which individuals with high myopia will develop pathological changes is still a huge challenge, so combining our data with established risk factors such as age, axial length, refractive error, BCVA, and choroidal thickness[4] and integrating these through AI-based models and deep learning algorithms could significantly enhance predictive accuracy, which can be validated through longitudinal studies [46–48]. Based on our findings, we infer that OCTA, which quantifies vascular abnormalities, and mfERG, which measures the photoelectric physiological responses of retinal cells, are complementary technologies. When used together, they can provide ophthalmologists and clinicians with a more comprehensive assessment of myopia progression, thereby supporting earlier, more effective, and individualized management strategies.

Limitations and future directions

This study has limitations that should be considered. First, the study's cross-sectional design limits the ability to establish causal relationships, and future longitudinal studies are needed. Second, the narrow age range of participants and the use of purposive sampling restrict the generalizability of findings across other age groups. The small sample size, which limits statistical power might have contributed to small AUC values in ROC curve analysis; future studies with larger and randomized sample may enhance predictive values.

AUC values between 0.7 and 0.8, as observed in this study, indicate good diagnostic ability, while values between 0.6 and 0.7 are considered average for disease detection. [49, 50] Therefore, we believe our ROC analysis of mfERG and OCTA can inform axial length elongation with fair discrimination ability. Finally, the exclusion of individuals with moderate and pathological myopia limits the applicability of our results to a broader spectrum of myopic conditions. These limitations underscore the need for more comprehensive research that encompasses a wider range of ages and myopia severities to provide a more complete understanding of the phenomenon being studied.

Conclusion

This study highlights a significant structural-functional relationship observed through OCTA and mfERG in individuals with high myopia in different retinal loci. In the foveal region, N1 implicit time, in the parafoveal region, SCP-VD and in the perifoveal region, DCP-VD, P1 implicit time and N1 implicit time demonstrated good capability in detecting myopic axial length elongation. The findings of this study can have implications in monitoring myopia progression and myopic retinal complications.

Data Availability Statement: Data and materials supporting this work will be provided upon request.

References

1. Fricke TR, Jong M, Naidoo KS, Sankaridurg P, Naduvilath TJ, Ho SM, et al. Global prevalence of visual impairment associated with myopic macular degeneration and temporal trends from 2000 through 2050: Systematic review, meta-analysis and modelling. Br J Ophthalmol. 2018;102(7):855–62.

2. Ang M, Wong TY. Updates on myopia: A clinical perspective. Updat Myopia A Clin Perspect. 2019;1–305.

3. B. A. Holden, S. P. Mariotti, I. Kocur, S. Resnikoff, H. Mingguang, K. Naidoo and MJ. The Impact of Myopia Impact of Increasing and Myopia Prevalenceof Myopia. World Heal Organ Holden Vis Inst. 2015;(March):1–40.

4. Gyawali P, Jnawali A, Kharal A, Subedi M, Kandel S, Puri PR, et al. SubFoveal Choroidal Imaging in High Myopic Nepalese Cohort. J Ophthalmol. 2023;2023:2209496.

5. Ismael ZF, El-Shazly AAEF, Farweez YA, Osman MMM. Relationship between functional and structural retinal changes in myopic eyes. Clin Exp Optom. 2017;100(6):695–703.

6. Zheng Q, Zong Y, Li L, Huang X, Lin L, Yang W, et al. Retinal vessel oxygen saturation and vessel diameter in high myopia. Ophthalmic Physiol Opt. 2015;35(5):562–9.

7. Mo J, Duan A, Chan S, Wang X, Wei W. Vascular flow density in pathological myopia: An optical coherence tomography angiography study. BMJ Open. 2017;7(2):1–7.

8. Yang YS, Koh JW. Choroidal Blood Flow Change in Eyes with High Myopia. Korean J Ophthalmol. 2015;29(5):309–14.

9. Park S, Kim SH, Park TK, Ohn YH. Evaluation of structural and functional changes

in non-pathologic myopic fundus using multifocal electroretinogram and optical coherence tomography. Doc Ophthalmol. 2013;126(3):199–210.

10. Jiang Y, Lou S, Li Y, Chen Y, Lu TC. High myopia and macular vascular density: an optical coherence tomography angiography study. BMC Ophthalmol [Internet]. 2021;21(1):1–5. Available from: https://doi.org/10.1186/s12886-021-02156-2

11. Benavente-Perez A. Evidence of vascular involvement in myopia: a review. Front Med. 2023;10(May).

12. Ng DSC, Chen LJ, Chan LKY, Tang FY, Teh WM, Zhou L, et al. Improved accuracy of spectral-domain optical coherence tomography and optical coherence tomography angiography for monitoring myopic macular neovascularisation activity. Br J Ophthalmol. 2024 May;

13. Hoffmann MB, Bach M, Kondo M, Li S, Walker S, Holopigian K, et al. ISCEV standard for clinical multifocal electroretinography (mfERG) (2021 update). Doc Ophthalmol [Internet]. 2021;142(1):5–16. Available from: https://doi.org/10.1007/s10633-020-09812-w

14. Gupta SK, Chakraborty R, Verkicharla PK. Electroretinogram responses in myopia: a review. Doc Ophthalmol [Internet]. 2021;145(2):77–95. Available from: https://doi.org/10.1007/s10633-021-09857-5

15. Veselinović M, Trenkić M, Čanadanović V, Jovanović P, Veselinović A, Petrović M, et al. The Significance of OCTA in Studying Vessel Density and Retinal Thickness in Individuals with Myopia. Med. 2025;61(3):1–15.

16. Ho WC, Kee CS, Chan HHL. Myopia progression in children is linked with reduced foveal mfERG response. Invest Ophthalmol Vis Sci. 2012 Aug;53(9):5320–5.

17. Zhang Y, Zhong Y, Mao W, Zhang Z, Zhou Y, Li H, et al. Clinical features evaluation of myopic fundus tessellation from OCTA and MfERG. Photodiagnosis Photodyn Ther. 2025;52(November 2024).

18. Munk MR, Giannakaki-Zimmermann H, Berger L, Huf W, Ebneter A, Wolf S, et al. OCT-angiography: A qualitative and quantitative comparison of 4 OCT-A devices. PLoS One. 2017;12(5):e0177059.

19. Mehta N, Liu K, Alibhai AY, Gendelman I, Braun PX, Ishibazawa A, et al. Impact of Binarization Thresholding and Brightness/Contrast Adjustment Methodology on Optical Coherence Tomography Angiography Image Quantification. Am J Ophthalmol. 2019 Sep;205:54–65.

20. Freedman IG, Li E, Hui L, Adelman RA, Nwanyanwu K, Wang JC. The Impact of Image Processing Algorithms on Optical Coherence Tomography Angiography Metrics and Study Conclusions in Diabetic Retinopathy. Transl Vis Sci Technol. 2022 Sep;11(9):7.

21. Zhang J, Tang FY, Cheung CY, Chen H. Different effect of media opacity on vessel density measured by different optical coherence tomography angiography algorithms. Transl Vis Sci Technol. 2020;9(8):1–9.

22. Le Boité H, Chetrit M, Erginay A, Bonnin S, Lavia C, Tadayoni R, et al. Impact of image averaging on vessel detection using optical coherence tomography angiography in eyes with macular oedema and in healthy eyes. PLoS One. 2021;16(10):e0257859.

23. Pramil V, Levine ES, Waheed NK. Macular vessel density in diabetic retinopathy patients: How can we accurately measure and what can it tell us? Clin Ophthalmol. 2021;15:1517–27.

24. Garway-Heath DF, Rudnicka AR, Lowe T, Foster PJ, Fitzke FW, Hitchings RA. Measurement of optic disc size: equivalence of methods to correct for ocular magnification. Br J Ophthalmol. 1998 Jun;82(6):643–9.

25. Sampson DM, Gong P, An D, Menghini M, Hansen A, Mackey DA, et al. Axial Length Variation Impacts on Superficial Retinal Vessel Density and Foveal

Avascular Zone Area Measurements Using Optical Coherence Tomography Angiography. Invest Ophthalmol Vis Sci. 2017 Jun;58(7):3065–72.

26. Dutt DDCS, Yazar S, Charng J, Mackey DA, Chen FK, Sampson DM. Correcting magnification error in foveal avascular zone area measurements of optical coherence tomography angiography images with estimated axial length. Eye Vis (London, England). 2022 Aug;9(1):29.

27. Sener H, Sevim DG, Oner A, Erkilic K. Correlation between optical coherence tomography angiography and multifocal electroretinogram findings in patients with diabetes mellitus. Photodiagnosis Photodyn Ther [Internet]. 2021;36(September):102558. Available from: https://doi.org/10.1016/j.pdpdt.2021.102558

28. Chamberlain P, Lazon de la Jara P, Arumugam B, Bullimore MA. Axial length targets for myopia control. Ophthalmic Physiol Opt J Br Coll Ophthalmic Opt. 2021 May;41(3):523–31.

29. Saunders KJ, McCullough SJ. Normative data for emmetropic and myopic eye growth in childhood. Vol. 41, Ophthalmic & physiological optics : the journal of the British College of Ophthalmic Opticians (Optometrists). England; 2021. p. 1382–3.

30. Shi Y, Ye L, Chen Q, Hu G, Yin Y, Fan Y, et al. Macular Vessel Density Changes in Young Adults With High Myopia: A Longitudinal Study. Front Med. 2021;8(June):1–10.

31. Min CH, Al-Qattan HM, Lee JY, Kim JG, Yoon YH, Kim YJ. Macular microvasculature in high myopia without pathologic changes: An optical coherence tomography angiography study. Korean J Ophthalmol. 2020;34(2):106–12.

32. Živković MLJ, Lazić L, Zlatanovic M, Zlatanović N, Brzaković M, Jovanović M, et al. The Influence of Myopia on the Foveal Avascular Zone and Density of Blood Vessels of the Macula—An OCTA Study. Med. 2023;59(3):1–10.

33. Birol G, Wang S, Budzynski E, Wangsa-Wirawan ND, Linsenmeier RA. Oxygen distribution and consumption in the macaque retina. Am J Physiol - Hear Circ Physiol. 2007;293(3).

34. Usui Y, Westenskow PD, Kurihara T, Aguilar E, Sakimoto S, Paris LP, et al. Neurovascular crosstalk between interneurons and capillaries is required for vision. J Clin Invest. 2015;125(6):2335–46.

35. Iafe NA, Phasukkijwatana N, Chen X, Sarraf D. Retinal capillary density and foveal avascular zone area are age-dependent: Quantitative analysis using optical coherence tomography angiography. Investig Ophthalmol Vis Sci. 2016;57(13):5780–7.

36. Steigerwalt RD, Cesarone MR, Belcaro G, Pascarella A, Rapagnetta L, Angelis M De, et al. Ocular Ischemia in High Myopia Treated With Intravenous Prostaglandin E1. Retin Cases Brief Rep. 2009;3(4):379–82.

37. Li KY, Tiruveedhula P, Roorda A. Intersubject variability of foveal cone photoreceptor density in relation to eye length. Invest Ophthalmol Vis Sci. 2010 Dec;51(12):6858–67.

38. Akhlaghi M, Kianersi F, Radmehr H, Dehghani A, Naderi Beni A, Noorshargh P. Evaluation of optical coherence tomography angiography parameters in patients treated with Hydroxychloroquine. BMC Ophthalmol. 2021;21(1):1–8.

39. Scarinci F, Nesper PL, Fawzi AA. Deep Retinal Capillary Nonperfusion Is Associated with Photoreceptor Disruption in Diabetic Macular Ischemia. Am J Ophthalmol [Internet]. 2016;168:129–38. Available from: http://dx.doi.org/10.1016/j.ajo.2016.05.002

40. Munk MR, Jampol LM, Souza EC, De Andrade GC, Esmaili DD, Sarraf D, et al. New associations of classic acute macular neuroretinopathy. Br J Ophthalmol. 2016;100(3):389–94.

41. Yoshikawa Y, Shoji T, Kanno J, Ishii H, Chino M, Igawa Y, et al. Relationship

Between Deep Retinal Macular Vessel Density and Bipolar Cell Function in Glaucomatous Eyes. Transl Vis Sci Technol. 2022;11(10):1–9.

42. Srinivasan S, Sivaprasad S, Rajalakshmi R, Anjana RM, Malik RA, Kulothungan V, et al. Assessment of optical coherence tomography angiography and multifocal electroretinography in eyes with and without nonproliferative diabetic retinopathy. Indian J Ophthalmol. 2021 Nov;69(11):3235–40.

43. Klemp K, Lund-Andersen H, Sander B, Larsen M. The effect of acute hypoxia and hyperoxia on the slow multifocal electroretinogram in healthy subjects. Investig Ophthalmol Vis Sci. 2007;48(7):3405–12.

44. Silva R. Myopic maculopathy: A review. Ophthalmologica. 2012;228(4):197–213.

45. Akyol N, Kükner AS, Ozdemir T, Esmerligil S. Choroidal and retinal blood flow changes in degenerative myopia. Can J Ophthalmol. 1996 Apr;31(3):113–9.

46. He X, Wang Y, Zhang X, Chi W, Yang W. Artificial intelligence in pathologic myopia: a review of clinical research studies. Front Med. 2025;12.

47. Ueta T, Makino S, Yamamoto Y, Fukushima H, Yashiro S, Nagahara M. Pathologic myopia: an overview of the current understanding and interventions. Glob Heal Med. 2020;2(3):151–5.

48. Hoang Q V., Flitcroft I, Rizzieri N. Can we predict which high myopes will develop pathological myopia? Ophthalmic Physiol Opt. 2025;45(4):906–10.

49. Jiménez-Valverde A. Sample size for the evaluation of presence-absence models. Ecol Indic [Internet]. 2020;114(March):106289. Available from: https://doi.org/10.1016/j.ecolind.2020.106289

50. Choi BC. Slopes of a receiver operating characteristic curve and likelihood ratios for a diagnostic test. Am J Epidemiol. 1998 Dec;148(11):1127–32.

Table 1: Demographic and Clinical characteristics of High myopes and Emmetropes

Demographic characteristics	High myope	Emmetrope	p-value
	Median (IQR)	Median (IQR)	
Age (years)	21.00(5.50)	23.00 (4.00)	0.23‡
Gender ratio (M: F)	23:17	16:24	0.18#
Spherical Equivalent (Dioptre)	-7.87 (2.38)	0.00 (0.00)	<0.001‡
Axial Length (mm)	26.19 (2.50)	23.12 (1.12)	<0.001‡
Keratometry (mm)	7.85 (0.67)	7.83 (0.55)	0.45‡

IQR: InterQuartile Range, M: Male, F: Female, MAR: Minimal Angle of Resolution, mm: Millimeter, BCVA: Best Corrected Visual Acuity

Chi-square test, ‡ Man Whitney U test

Table 2: Comparision of retinal vessel density parameters between High myopes and Emmetropes

OCTA Parameters (Retinal Vessel Density)	Retinal Zones	High Myopia	Emmetrope	Mean difference (SD) between high myopes and emmetropes	p Value
		Mean (SD)	Mean (SD)		
SCP-VD (%)	Foveal	17.95(6.05)	23.18(6.53)	-5.23 (1.42)	<0.001 ** §
	Para Foveal	49.39(5.15)	54.63(4.28)	-5.24 (1.05)	<0.001 ** §
	Peri Foveal	48.03(4.47)	52.19(3.49)	-4.16 (0.89)	<0.001** §
DCP-VD (%)	Foveal	35.17(7.89)	39.16(8.60)	-3.99 (1.86)	0.05*§
	Para Foveal	53.96(5.24)	59.44(4.47)	-5.48 (1.08)	<0.001 ** §
	Peri Foveal	45.69(7.91)	57.36(6.51)	-11.67 (1.61)	<0.001** §

** Significance at 0.01 level or less (2-tailed),* Significance at 0.05 level (2-tailed)

§ Independent Sample-t test, SD: Standard Deviation, SCP-VD:Superficial Capillary Plexus Vessel Density, DCP-VD: Deep Capillary Plexus Vessel Density

Table 3: Comparision of mfERG parameters between High myopes and Emmetropes

mfERG parameters	Rings	High Myopes	Emmetropes	Mean difference (SD) between High Myopia and Emmetropia	p Value
		Mean (SD)	Mean (SD)		
P1 Amplitude (μV/degree^2)	Ring 1	51.13 (10.86)	67.19 (14.30)	-16.06 (2.84)	<0.001** §
	Ring 2	34.46 (8.64)	46.28 (9.35)	-11.82 (2.01)	<0.001 **§
	Ring 3	26.13(6.72)	32.67 (6.46)	-6.54 (1.47)	<0.001 **§
P1 Implicit Time (millisec)	Ring 1	52.07 (3.69)	49.17(3.12)	2.90 (0.76)	<0.001**§
	Ring 2	48.70(2.02)	46.01(1.35)	2.69 (0.38)	<0.001**§
	Ring 3	46.81(1.46)	45.00(1.07)	1.81 (0.29)	<0.001**§
N1# Amplitude (μV/degree^2)	Ring 1	-31.01(6.53)	-43.77(7.41)	-12.76 (1.56)	<0.001**§
	Ring 2	-20.34(4.53)	-25.03(7.47)	-4.69 (1.38)	<0.001**§
	Ring 3	-15.11(4.01)	-17.38(4.16)	-2.27 (0.91)	0.01 * *‡
N1 Implicit Time (milisec)	Ring 1	26.62(3.09)	24.68(2.47)	1.94 (0.62)	<0.001**§
	Ring 2	28.25(2.24)	26.35(1.48)	1.90 (0.43)	<0.001**‡
	Ring 3	28.05(1.77)	26.30(1.08)	1.75 (0.33)	<0.001**‡

** Significance at 0.01 level or less (2-tailed), * Significance at 0.05 level (2-tailed)

Man Whitney U ‡, Independent Sample t test§, SD: Standard Deviation

For N1 amplitude negative sign indicate downward deflection of wave and we only consider magnitude

Table 4: Topographical correlation between mfERGparameters with Retinal Vessel Density Parameters in Emmetropes

Spearman's Rank Correlation		SCP-VD	DCP-VD
		r (p value)	r (p value)
Correlation between P1 Amplitude And Vessel Density	Ring 1Amplitude With Foveal Density	0.19 (0.22)	0.11 (0.51)
	Ring 2 Amplitude With Parafoveal Density	0.06(0.67)	0.03(0.87)
	Ring 3 Amplitude With Perifoveal Density	0.06 (0.97)	0.11 (0.49)
Correlation Between P1 Implicit Time And Vessel Density	Ring 1Implicit Time With Foveal Density	-0.14(0.39)	-0.09(0.59)
	Ring 2 Implicit Time With Para Foveal Density	-0.13 (0.43)	-0.09 (0.58)
	Ring 3 Implicit Time With Peri Foveal Density	-0.14(0.40)	-0.16 (0.34)
Correlation between N1 Amplitude And Vessel Density	Ring 1 Amplitude With Foveal Density	0.06(0.70)	0.02(0.88)
	Ring 2 Amplitude With Para Foveal Density	0.06 (0.71)	0.08 (0.60)
	Ring 3 Amplitude With Peri Foveal Density	0.07 (0.66)	0.04 (0.81)
Correlation Between N1 Implicit Time And Vessel Density	Ring 1Implicit Time With Foveal Density	-0.11 (0.48)	-0.16(0.31)
	Ring 2 Implicit Time With Para Foveal Density	-0.17 (0.29)	-0.10 (0.54)
	Ring 3 Implicit Time With Peri Foveal Density	-0.07 (0.68)	-0.07 (0.68)

** Correlation is significant at the 0.01 level (2-tailed),
* Correlation is significant at the 0.05 level (2-tailed).

SCP-VD: Superficial Capillary Plexus Vessel Density, DCP-VD: Deep Capillary Plexus Vessel Density

Table 5: Topographical correlation between mfERGparameters with Retinal Vessel Density Parameters in High Myopes

Spearman's Rank Correlation (HIGH MYOPES)		SCP-VD	DCP-VD
		r (p value)	r (p value)
Correlation between P1 Amplitude And Vessel Density	Ring 1Amplitude and With Foveal Density	0.24 (0.16)	0.36 (0.23)
	Ring 2 Amplitude With Parafoveal Density	**0.34(0.03) ***	**0.58(<0.001) ****
	Ring 3 Amplitude With Perifoveal Density	**0.40 (0.01) ***	0.29(0.07)
Correlation Between P1 Implicit Time And Vessel Density	Ring 1Implicit Time With Foveal Density	-0.19(0.23)	-0.25 (0.12)
	Ring 2 Implicit Time With Para Foveal Density	-0.03 (0.84)	-0.05(0.77)
	Ring 3 Implicit Time With Peri Foveal Density	-0.23(0.15)	-0.03(0.88)
Correlation between N1 Amplitude And Vessel Density	Ring 1 Amplitude With Foveal Density	0.16(0.32)	0.20(0.22)
	Ring 2 Amplitude With Para Foveal Density	0.22 (0.16)	**0.34 (0.03) ****
	Ring 3 Amplitude With Peri Foveal Density	**0.36 (0.02) ***	**0.36 (0.02) ***
Correlation Between N1 Implicit Time And Vessel Density	Ring 1Implicit Time With Foveal Density	-0.04 (0.82)	-0.03 (0.84)
	Ring 2 Implicit Time With Para Foveal Density	-0.11 (0.51)	-0.11(0.52)
	Ring 3 Implicit Time With Peri Foveal Density	-0.13 (0.41)	-0.17 (0.27)

** Correlation is significant at the 0.01 level (2-tailed),
* Correlation is significant at the 0.05 level (2-tailed).

SCP-VD: Superficial Capillary Plexus Vessel Density, DCP-VD: Deep Capillary Plexus Vessel Density

Table 6: Multiple linear regression analyses of factors associated with mfERGparametersin high myopes.

	Multiple linear regression								
	Explanatory Variables Model 1					Explanatory Variables Model 2 (Excluding Age)			
Dependent Variable	R^2	Age	Axial length	SCP-VD	DCP-VD	R^2	Axial length	SCP-VD	DCP-VD
	[β (95 % CI), p value]					[β (95 % CI), p value]			
Ring 1 P1 Amplitude	0.22	[-0.56 (-1.62, 0.51), 0.30]	**[-3.29 (-4.96,-1.63), <0.001**]**	[-0.14 (-0.98, 0.69), 0.73] §	[0.27 (-0.36, 0.90), 0.39] §	0.21	**[-3.24(-4.90,-1.580, <0.01*]**	[-0.18(-1.01,0.65), 0.66] §	[0.29(-0.34, 0.92), 0.35] §
Ring 2 P1 Amplitude	0.47	[-0.67 (-1.31,-0.02),0.06]	**[-2.59 (-3.78, -1.41), <0.001**]**	**[-0.69 (-1.21, -0.17), 0.03*]** ¶	**[1.02 (0.53, 1.52), <0.001**]** ¶	0.44	**[-2.45(-3.641, -1.249), <0.01*]**	**[-0.57(-1.085, -0.047), 0.03]** ¶	**[0.94(-0.44,1.44), <0.001**]** ¶
Ring 3 P1 Amplitude	0.27	[-0.27(-0.82, 0.28),0.33]	**[-1.21 (-2.22, -0.20), 0.02*]**	[-0.08 (-0.58, 0.42), 0.75] †	[0.18 (-0.05, 0.48), 0.11] †	0.26	**[-1.17 (-2.17, 0.16), 0.02*]**	[0.02 (-0.44, 0.48), 0.93] †	**[0.17 (-0.07, 0.43), 0.17]** †
Ring 1 N1 Amplitude	0.33	[0.31(-0.31,0.93),0.33]	**[-2.58(-1.60, -3.50), <0.001**]**	[-0.17(-0.67,0.31), 0.46] §	[0.13(-0.24,0.50), 0.47] §	0.32	**[-2.55(-3.55,-1.57),<0.01*]**	[-0.61(-1.13, -0.08), 0.25] §	[0.27(-0.16, 0.69), 0.21] §
Ring 2 N1 Amplitude	0.18	[-0.20(- 0.70, 0.29), 0.42]	[-0.60(-1.55,0.25), 0.16]	[-0.07(0.47,0.33), 0.72] ¶	**[0.36(0.01,0.76), 0.04*]** ¶	0.17	[-0.60(-1.49,0.29),0.18]	[0.04(-0.42,0.35), 0.85] ¶	**[0.35(-0.02, 0.72), 0.04*]** ¶
Ring 3 N1 Amplitude	0.26	[0.17 (-0.513,0.18), 0.30]	**[-1.17 (-2.17, 0.16), 0.02*]**	[0.02 (-0.44, 0.48), 0.93] †	[0.18(-0.08, 0.43), 0.17] †	0.26	**[-1.17(-2.16,0.16),0.02*]**	[0.02 (-0.44, 0.48), 0.92] †	**[0.17(-0.07, 0.43), 0.17]** †
Ring 1 P1 Implicit time	0.11	[-0.01(-0.29,0.26),0.91]	**[0.63(0.19, 1.06),0.01**]**	[0.04(-0.18,0.26),0.71] §	[-0.03(-0.194,0.14),0.75] §	0.10	**[0.63(0.19,1.06),0.01**]**	[0.04(-0.17,0.25),0.71] §	[-0.03(-0.19,0.14), 0.75] §
Ring 2 P1 Implicit time	0.33	[-0.01(-0.15,0.14),0.95]	**[0.69(0.42, 0.96), <0.001**]**	[0.03(-0.09, 0.15), 0.59] ¶	[0.01 (-0.10, 0.12), 0.86] ¶	0.33	**[0.69(0.42,0.95),<0.01*]**	[0.03(-0.08, 0.15), 0.57] ¶	[0.01(-0.10, 0.12), 0.86] ¶
Ring 3 P1 Implicit time	0.40	[0.01(-0.01, 0.12),0.81]	**[0.53 (0.34, 0.73), <0.001**]**	[-0.06(-0.16, 0.04),0.22] †	[0.05(-0.01,0.10),0.10] †	0.39	**[0.53(0.34,0.73),<0.01*]**	[-0.06 (-0.15,0.02),0.14] †	[0.05(-0.01,0.09), 0.07] †
Ring 1 N1 Implicit time (R^2 = 0.22)	0.14	[-0.04(-0.26,0.18),0.72]	**[0.58(0.24,0.92), <0.001**]**	[0.09(-0.08,0.26),0.32] §	[-0.06(-0.19,0.07),0.38] §	0.14	**[0.58(0.24,0.92),<0.01*]**	[0.02(-0.08,0.25),0.99] §	[-0.06(-0.18,0.07), 0.72] §
Ring 2 N1 Implicit time	0.29	[0.01 (-0.14, 0.16),0.92]	**[0.70 (0.44, 0.97), <0.001**]**	[0.03 (-0.08 0.15), 0.59] ¶	[0.09(-0.02,0.20), 0.11] ¶	0.29	**[0.70(0.44,0.97),<0.01*]**	[0.03(-0.08,0.14),0.58] ¶	[0.09(-0.02,0.2), 0.11] ¶

(R^2 = 0.22)									
Ring 3 N1 Implicit time (R^2 = 0.22)	0.39	[-0.04 (-0.15, 0.08),0.54]	**[0.52 (0.30, 0.73), <0.001**]**	[-0.06 (-0.17, 0.05), 0.26] †	[0.03 (-0.03, 0.08), 0.39] †	0.38	**[0.52(0.30,0.73),<0.01*]**	[-0.05(-0.14, 0.05), 0.33] †	[0.02(-0.03, 0.07), 0.47] †

** Significance at 0.01 level or less (2-tailed) * Significance at 0.05 level (2-tailed)

§ Foveal vessel density ¶ Para foveal density † Perifoveal vessel density

SCP-VD = Superficial Capillary Plexus Vessel Density, DCP-VD = Deep Capillary Plexus Vessel Density, , CI= Confidence Interval

Table 7: Multiple linear regression analyses of factors associated with superficial and deep capillary plexus vessel densities (SCP-VD and DCP-VD) at foveal, parafoveal and perifoveal zones in high myopes

Multiple Linear Regression						
Dependent Variable						
Explanatory Variables	SCP-VD (Foveal)			DCP-VD(Foveal)		
	R^2 Value	β (95 % CI)	p value	R^2 Value	β(95 % CI)	p value
Age	0.16	0.12(-0.37, 0.62)	0.62	0.06	0.02(-0.63,0.67)	0.94
Axial Length		**-1.33(-2.03, -0,63)**	**<0.001****		**-1.04(-1.97, -0.12)**	**0.03***

Explanatory Variables	SCP-VD (Para foveal)			DCP-VD (Para foveal)		
	R^2 Value	β (95 % CI)	p value	R^2 Value	β (95 % CI)	p value
Age	0.38	-0.25(-0.58,0.09)	0.14	0.36	0.06(-0.29,0.41)	0.73
Axial Length		**-1.65(-2.12, -1.17)**	**<0.001****		**-1.66(-2.16, -1.16)**	**<0.001****

Explanatory Variables	SCP-VD (Peri foveal)			DCP-VD (Peri foveal)		
	R^2 Value	β (95 % CI)	p value	R^2 Value	β (95 % CI)	p value
Age	0.39	-0.40(-0.68, 0.12)	- 0.05	0.48	0.15(-0.37,0.68)	0.56
Axial Length		**-1.32(-1.71, 0.92)**	**- <0.001****		**-3.18(-3.93, 2.43)**	**- <0.001****

** Significance at 0.01 level or less (2-tailed) * Significance at 0.05 level (2-tailed)

SCP-VD = Superficial Capillary Plexus Vessel Density, DCP-VD = Deep Capillary Plexus Vessel Density, CI= Confidence Interval

Table 8: ROC curve analysis of various OCTA and mfERG parameters in tracking axial length elongation

Retinal Zone	AUC± 2 SD	95% CI	Sensitivity (%)	Specificity (%)
SCP-VD (Foveal)	0.593± 0.074	(0.452-0.732)	73.7	43.5
DCP-VD (Foveal)	0.596± 0.073	(0.450-0.730)	77.2	39.1
P1 Amplitude (Ring 1)	0.608±0.063	(0.488-0.734)	31.6	95.7
N1 Amplitude (Ring 1)	0.593± 0.067	(0.459-0.727)	45.6	78.3
P1 Implicit time (Ring 1)	0.575±0.072	(0.434-0.709)	43.9	69.6
N1 Implicit time (Ring 1)	0.701 ±0.066	(0.571-0.826)	56.1	78.3
SCP-VD (Parafoveal)	0.693± 0.07	(0.542-0.828)	75.0	80.0
DCP-VD (Parafoveal)	0.643±0.071	(0.493-0.781)	78.0	82.0
P1 Amplitude (Ring 2)	0.664±0.07	(0.525-0.795)	72.5	78.0
N1 Amplitude (Ring 2)	0.653±0.069	(0.525-0.789)	68.0	73.0
P1 Implicit time (Ring 2)	0.671±0.06	(0.534-0.805)	77.0	85.0
N1 Implicit time (Ring 2)	0.680±0.074	(0.531-0.811)	70.0	80.0
SCP-VD (Perifoveal)	0.683± 0.073	(0.531-0.819)	59.6	78.3

DCP-VD (Perifoveal)	0.710±0.069	(0.566-0.841)	75.4	65.2
P1 Amplitude (Ring 3)	0.600± 0.072	(0.456-0.745)	49.1	69.6
N1 Amplitude (Ring 3)	0.586±0.071	(0.454-0.730)	57.9	65.2
P1 Implicit time (Ring 3)	0.704± 0.070	(0.566-0.830)	63.2	73.9
N1 Implicit time (Ring 3)	0.708± 0.072	(0.571-0.848)	78.9	60.9
	SCP-VD = Superficial Capillary Plexus Vessel Density, DCP-VD = Deep Capillary Plexus Vessel Density, AUC: Area Under Curve, CI: Confidence Interval			

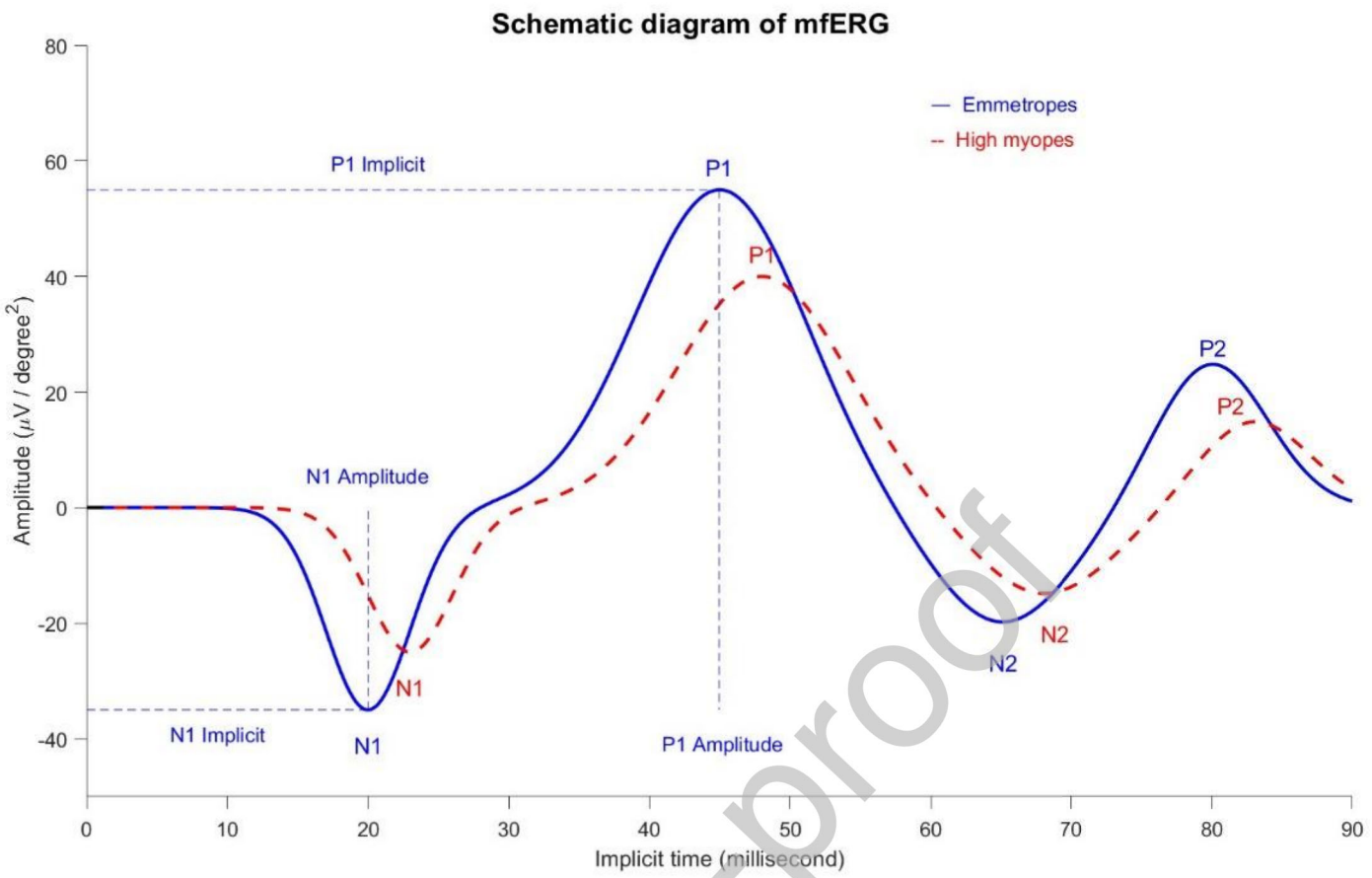

Figure 1: Schematic diagram of mfERG waveform and comparison of waveform between high myopes and emmetropes

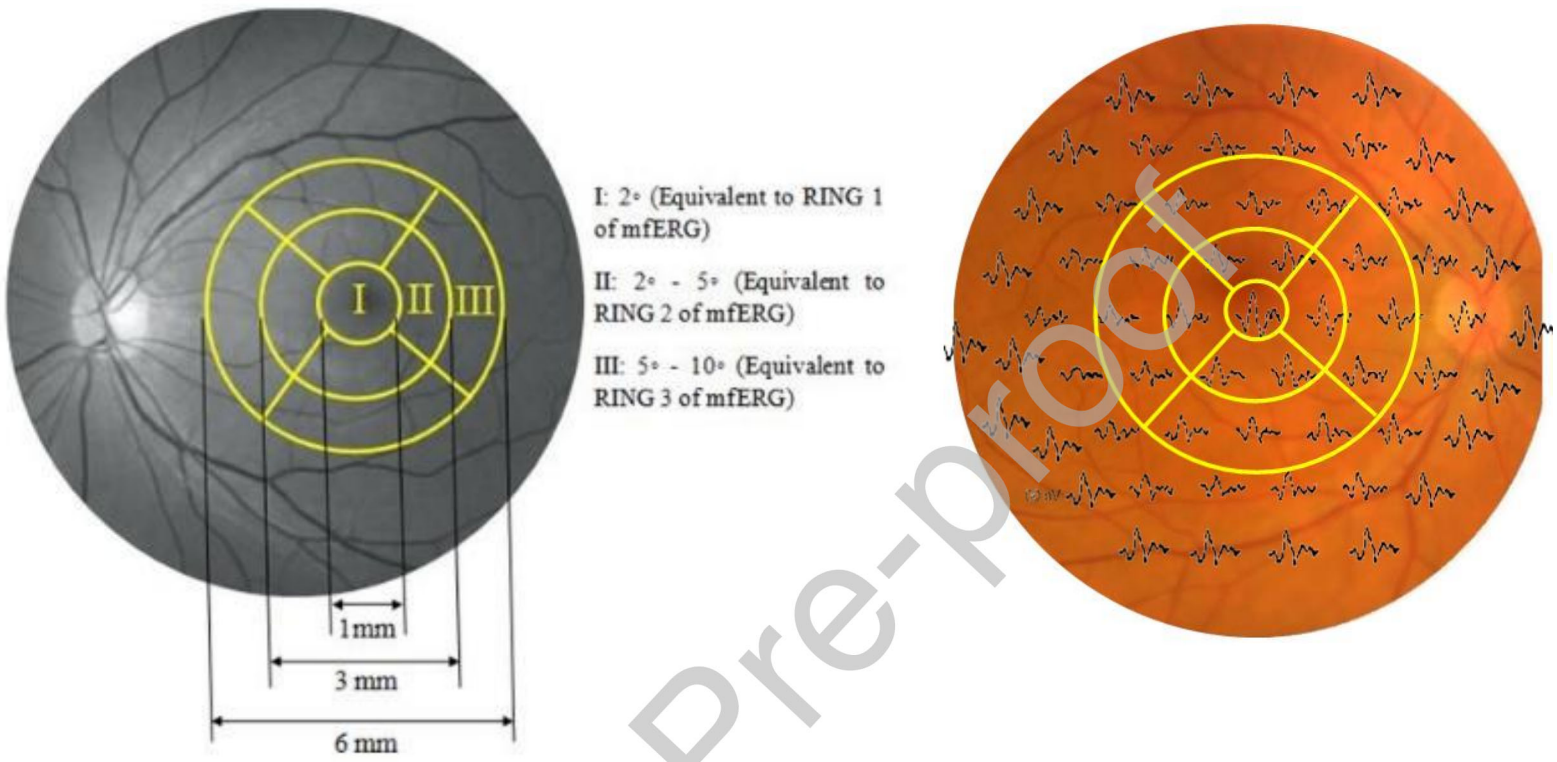

2A 2B

Figure 2A: Dimension of macula based on ETDRS map; **2B:** Topographical matching of ETDRS grid of OCTA with mfERG rings

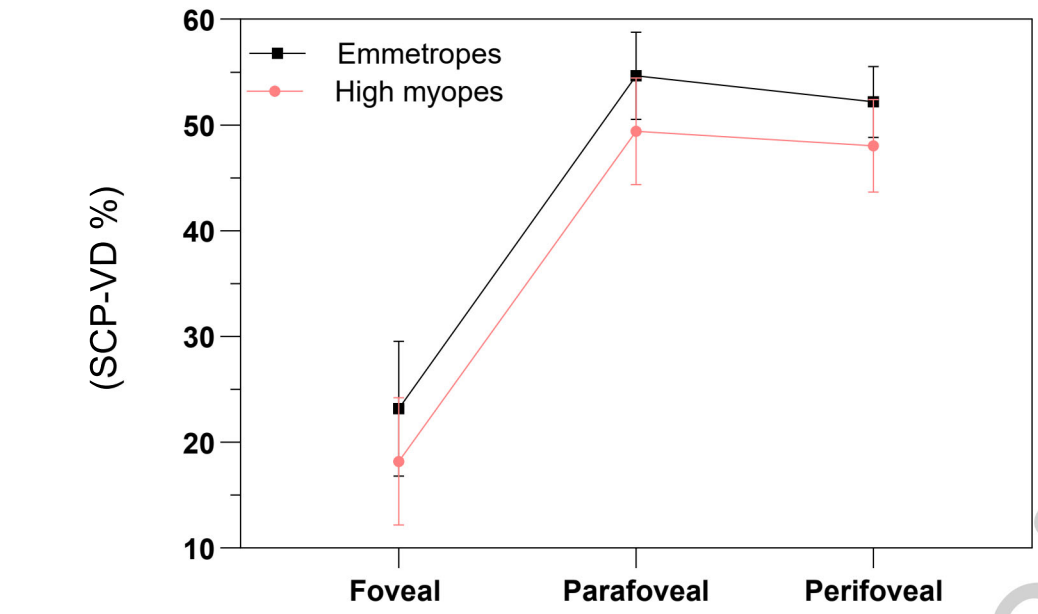

3A.

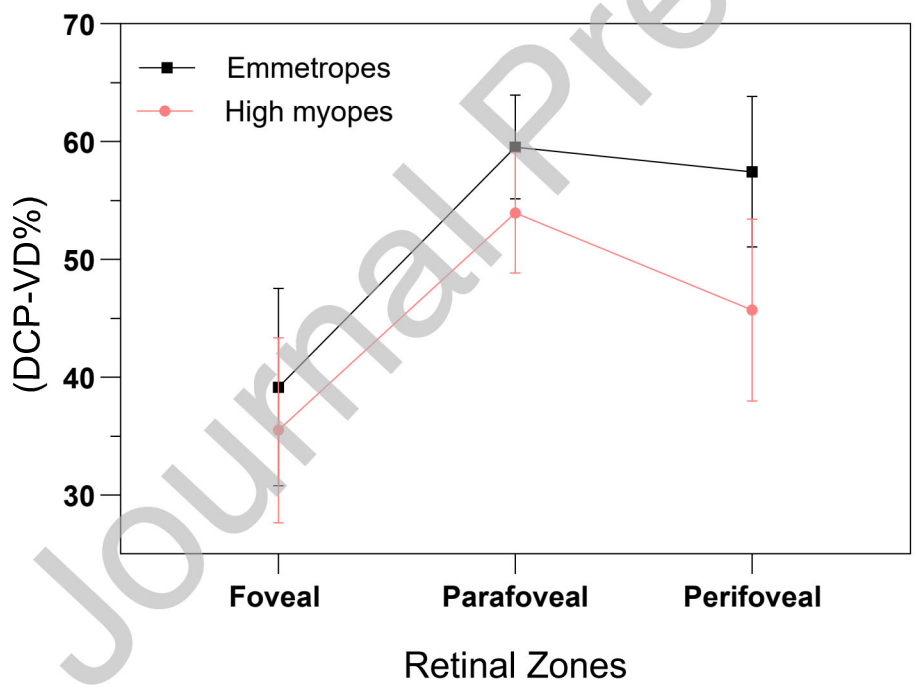

3B.

Figure 3A: Line graph comparing the Superficial Capillary Plexus Vessel Density (SCP-VD) at three retinal zones between High Myopia and Emmetrope; **3B:** Line graph comparing the Deep Capillary Plexus Vessel Density (DCP-VD) at three retinal zones between High Myopia and Emmetrope

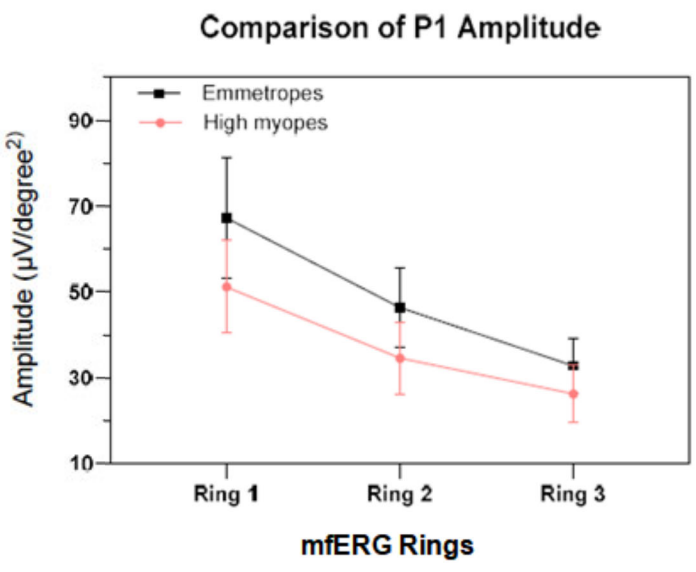

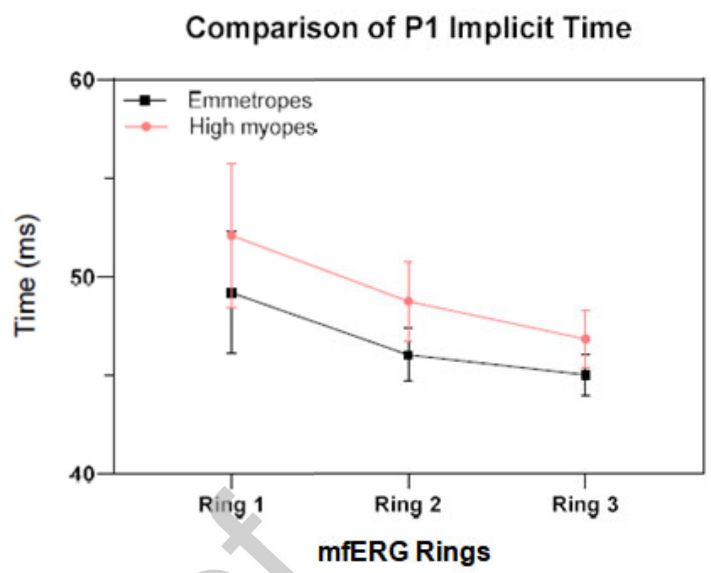

4A. 4B.

Figure 4A: Line graph comparing the mfERG P1 Amplitude at retinal zones between High Myopesand Emmetropes**; 4B:** Line graph comparing the mfERG P1 Implicit Time at retinal zones between High Myopes and Emmetropes

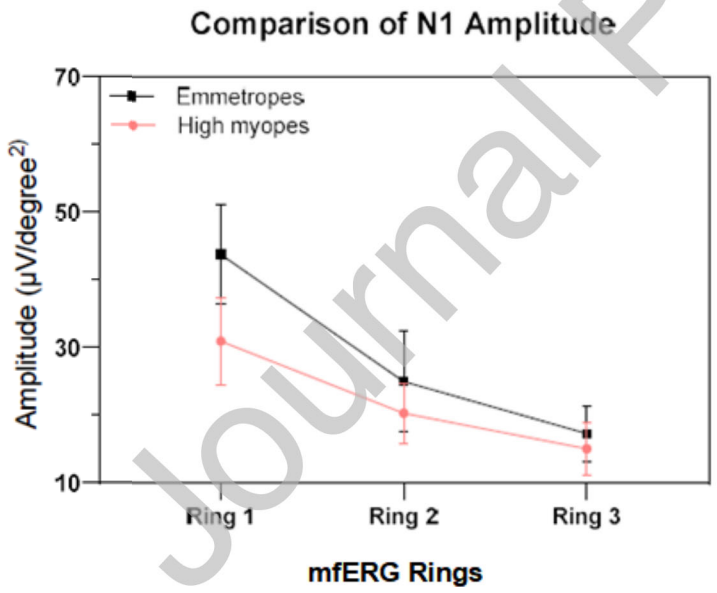

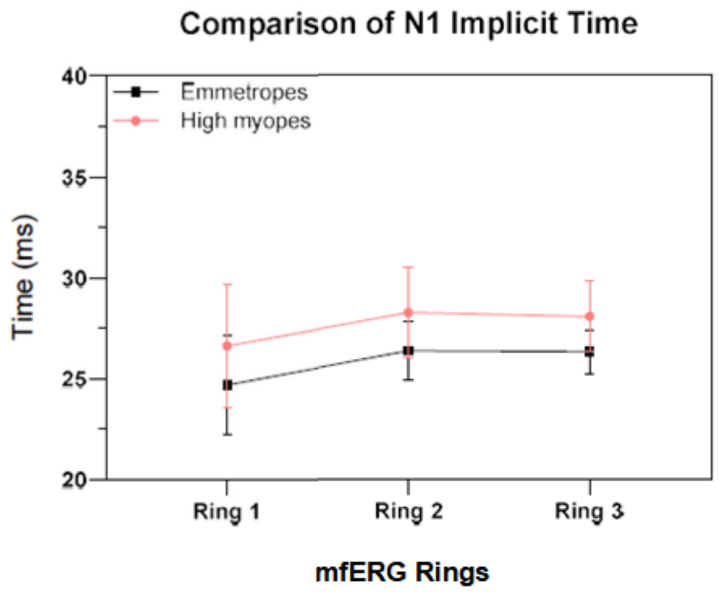

. 5A. 5B.

Figure 5A: Line graph comparing the mfERG N1 Amplitude at retinal zones between High Myopes and Emmetropes**; 5B:** Line graph comparing the mfERG N1 Implicit Time at retinal zones between High Myopes and Emmetropes

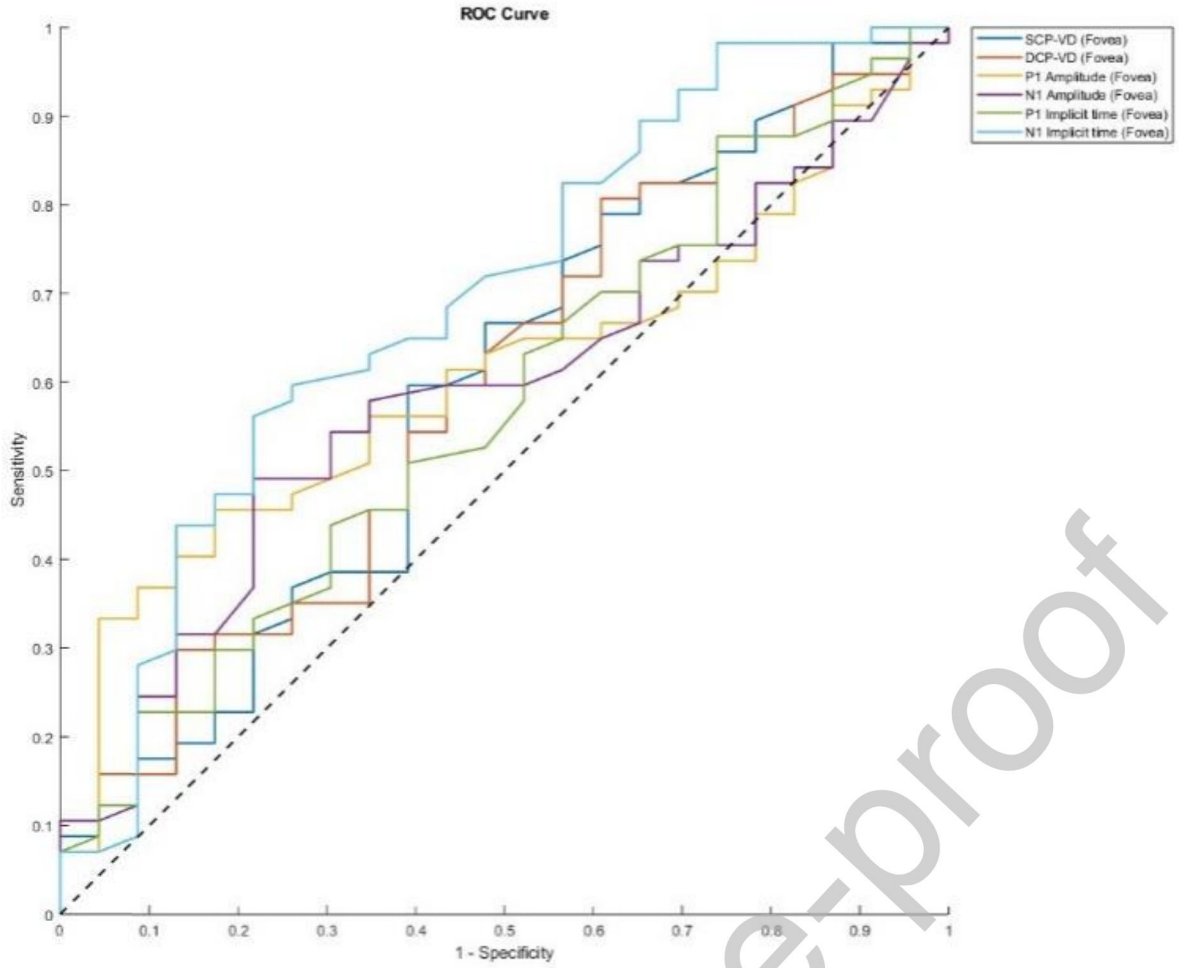

6A.

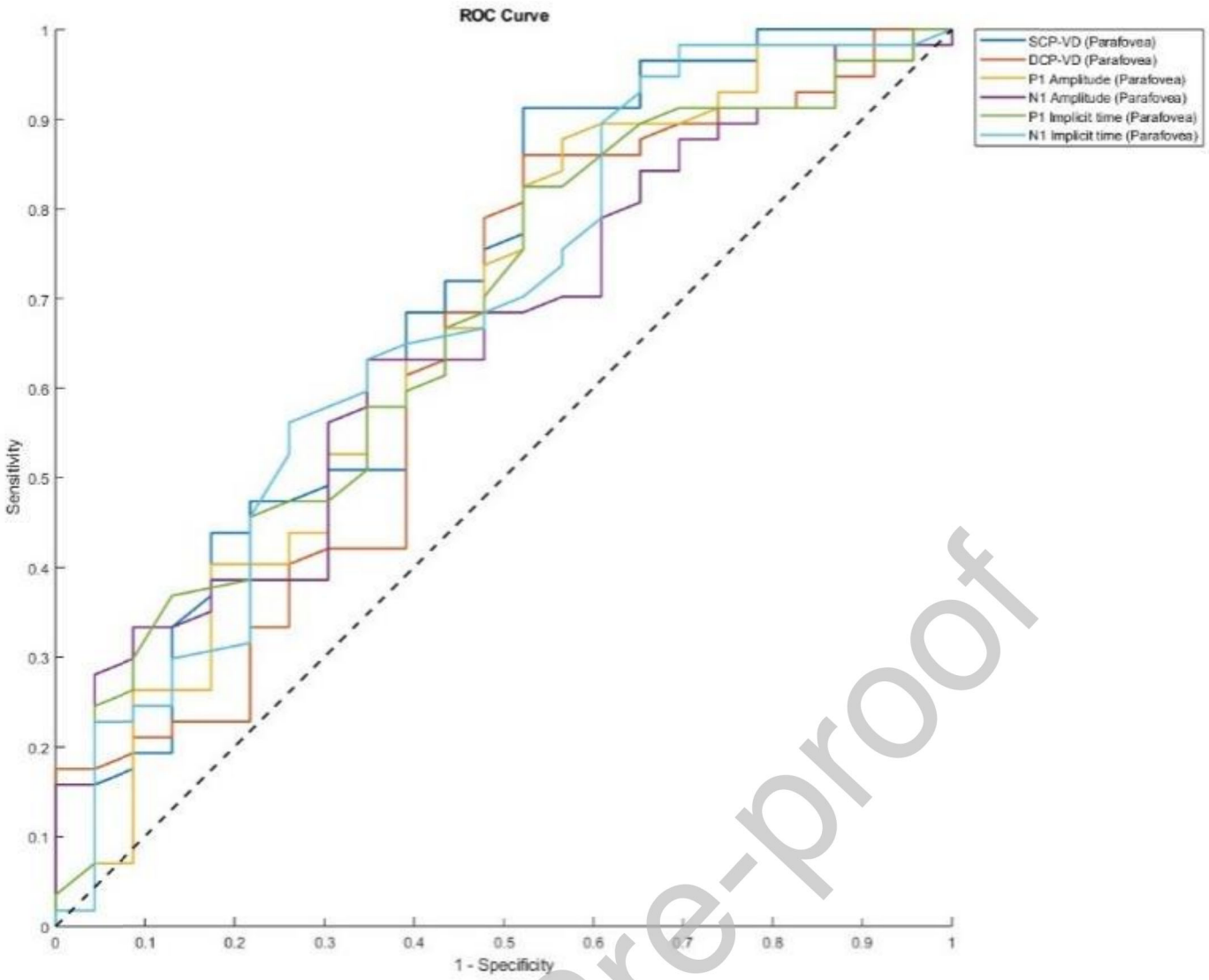

6B.

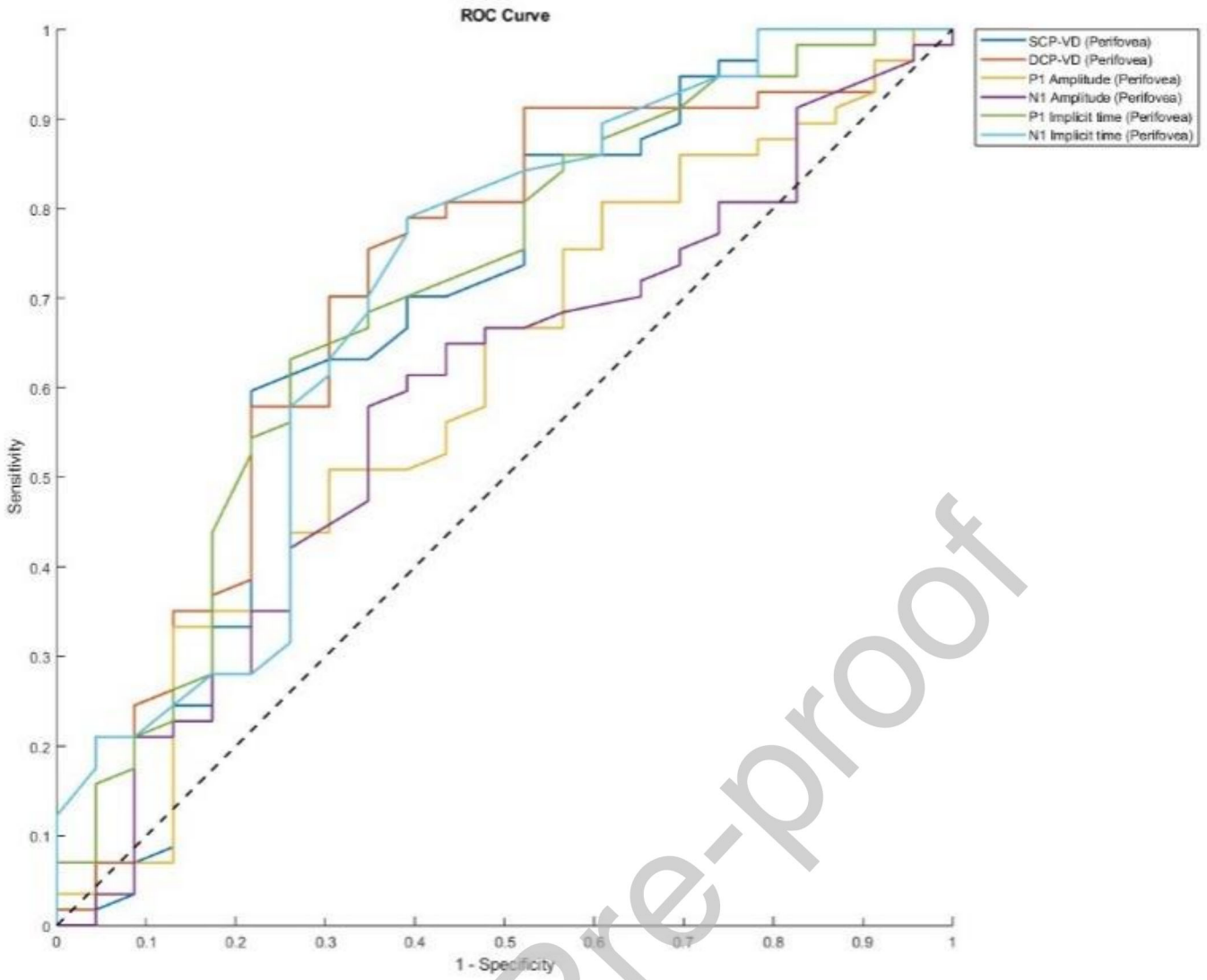

6C.

Figure 6: Receiver operating characteristics curve of mfERG (P1 amplitude, N1 amplitude, P1 implicit time and N1 implicit time) and OCTA(SCP-VDand DCP-VD) parameters for tracking criterionincrease in axial length of 0.1 mm in high myopes; **A:** foveal; **B:** parafoveal and **C:** perifoveal regions. Abbreviations: SCP-VD, superficial capillary plexus-vessel density and DCP-VD, deep capillary plexus-vessel density